Molecular Cell, Volume *75*

Supplemental Information

RPA Phosphorylation Inhibits DNA Resection

Michael M. Soniat, Logan R. Myler, Hung-Che Kuo, Tanya T. Paull, and Ilya J. Finkelstein

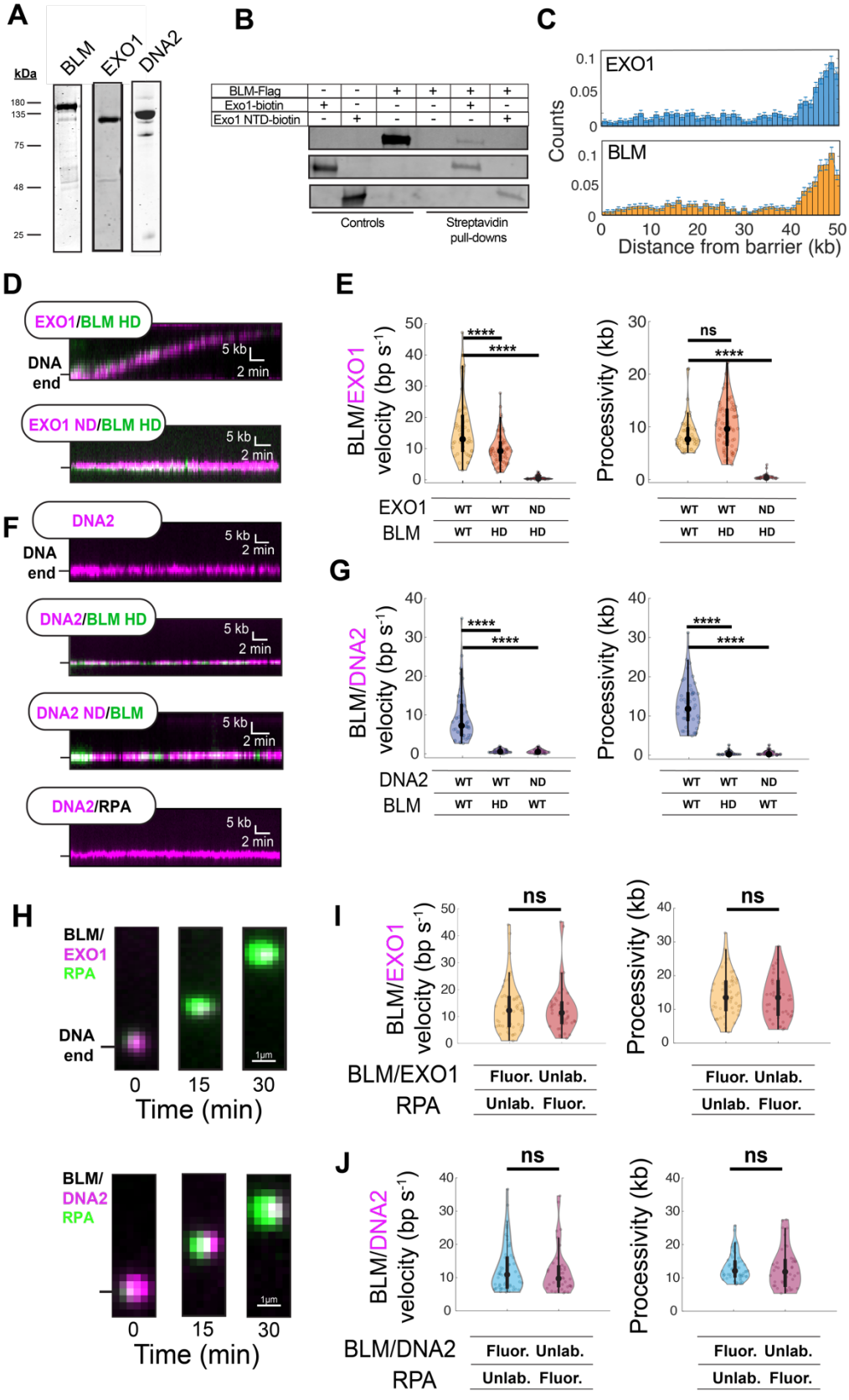
A
kDa
BLM
EXO1
DNA2
180
135
75
48
25
B
BLM-Flag
Exo1-biotin
Exo1 NTD-biotin
Controls
Streptavidin pull-downs
C
EXO1
BLM
Counts
Distance from barrier (kb)
D
EXO1/BLM HD
EXO1 ND/BLM HD
DNA end
5 kb
2 min
E
BLM/EXO1 velocity (bp s-1)
Processivity (kb)
****
ns
EXO1
BLM
WT WT ND
WT HD HD
F
DNA2
DNA2/BLM HD
DNA2 ND/BLM
DNA2/RPA
G
BLM/DNA2 velocity (bp s-1)
DNA2
BLM
H
BLM/
EXO1
RPA
DNA end
1μm
0 15 30
Time (min)
BLM/
DNA2
RPA
I
BLM/EXO1
RPA
Fluor. Unlab.
Unlab. Fluor.
J
BLM/DNA2

Figure S1. Characterization of BLM/EXO1 and BLM/DNA2 resectosomes, Related to Figure 1.

(A) SDS-PAGE gel of recombinant full-length BLM, EXO1, and DNA2. **(B)** Streptavidin pull-down assays showing BLM interacts with full-length EXO1 (lane 5) but not with the 352 amino acid N-terminal EXO1 catalytic domain (NTD; lane 6). **(C)** Histogram of BLM and EXO1 binding along the DNA substrate. BLM and EXO1 co-localize at the free DNA ends. Error bars are the SD as determined by bootstrapping. **(D)** Representative kymograph showing that helicase-dead (HD) BLM(K695A)/EXO1 is still able to resect DNA (n=78). In contrast, the helicase-dead BLM in complex with nuclease-dead (ND) EXO1 (D78A/D173A) binds but does not leave the DNA ends (n=40). **(E)** Velocity and processivity of the indicated catalytically inactive BLM and EXO1 complexes. **(F)** Representative kymographs showing that helicase-dead BLM(HD)/DNA2 (n=30) and nuclease-dead BLM/DNA2(ND) (n=30) are not able to resect DNA. In addition, neither DNA2 (n=30) nor DNA2/RPA (n=60) are able to catalyze long-distance DNA resection in the absence of BLM. **(G)** Velocity and processivity of BLM(HD)/DNA2 and BLM/DNA2(ND). **(H)** RPA-GFP (green) intensity increased with BLM/EXO1 and BLM/DNA2 resection due to accumulation of ssDNA EXO1 or DNA2 are shown in magenta. **(I-J)** Velocity and processivity of fluorescent and unlabeled **(I)** BLM/EXO1 (n=52 for fluorescent BLM/EXO1; n=40 for unlabeled BLM/EXO1) and **(J)** BLM/DNA2 (n=58 for fluorescent BLM/DNA2; n=40 for unlabeled BLM/DNA2) resectosomes. RPA-GFP was used to track resection with unlabeled resectosomes. The fluorescent and unlabeled resectosomes are statistically indistinguishable, indicating that fluorescent labeling does not interfere with enzyme function.

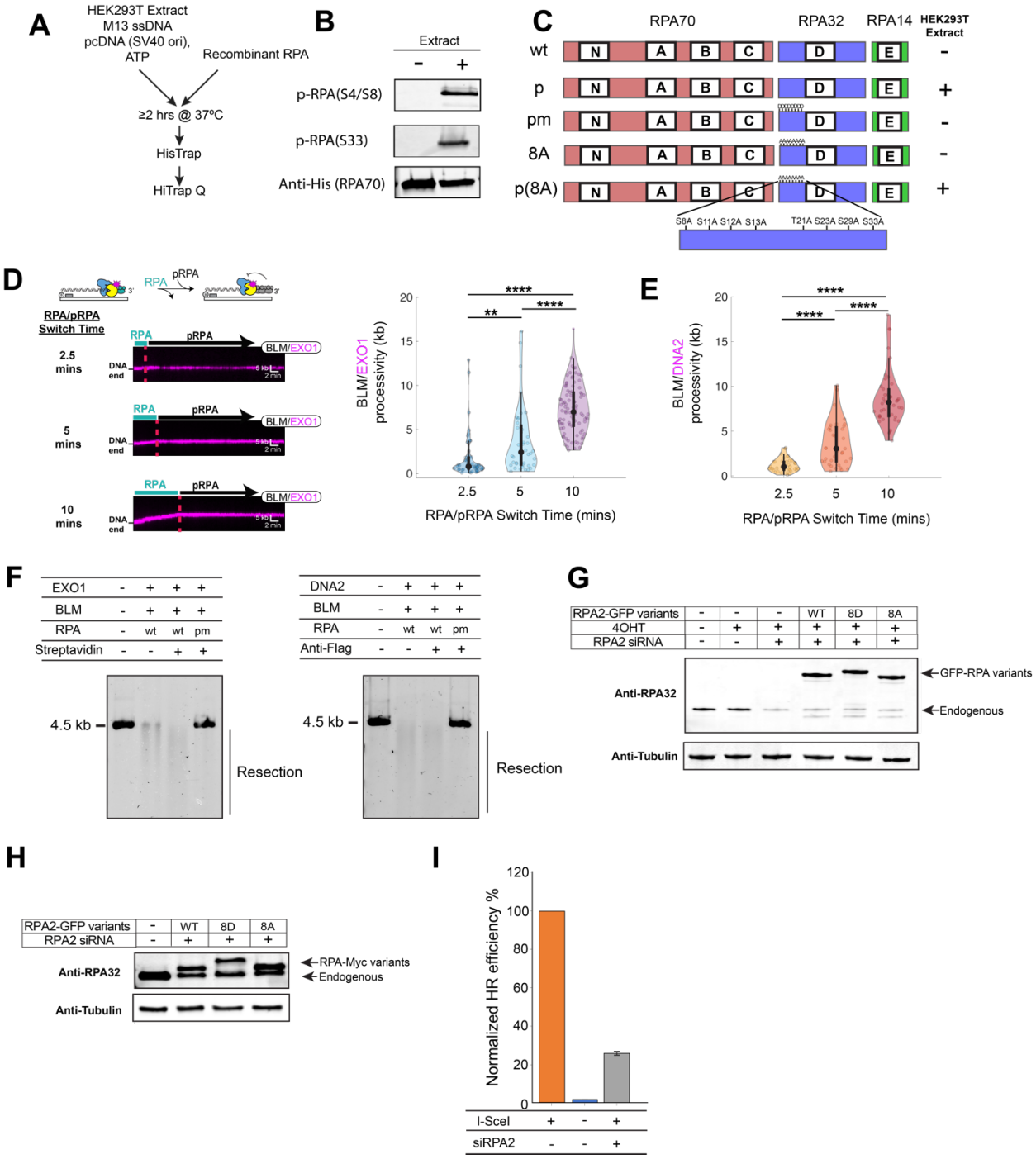

Figure S2. Phosphorylated RPA (pRPA) and its effect on DNA resection, Related to Figure 1.

(A) Schematic of the *in vitro* RPA phosphorylation protocol. **(B)** Western blot monitoring pS4/S8 and pS33 of recombinant pRPA with and without the addition of HEK293T extract. **(C)** Schematic of the RPA variants used in this study. **(D)** Representative kymographs (left) and processivity

(right) of BLM/EXO1 complexes resecting DNA in the presence of 1 nM RPA for 2.5 (n=25), 5 (n=25), and 10 (n=25) minutes prior to switching to pRPA for 40 minutes. **(E)** Processivity of BLM/DNA2 complexes under the same conditions as in (D). The dot in the violin plots represents the median and black bars indicate the interquartile range (thick bars) and 95% confidence intervals (thin bars) of the distributions. **(F)** Resection assays with EXO1 (1 nM), BLM (10 nM), DNA2 (10 nM), and RPA (100 nM) or pmRPA (100 nM). These data show that pmRPA inhibits resection. Inclusion of 1 μg of streptavidin (used for labeling EXO1) or anti-FLAG (for labeling DNA2) does not inhibit resection. Proteins were incubated with 30 ng of linearized 4.4-kb DNA (4-nt 3' overhang) for 30 min at 37°C. Resected DNA was separated on a 1% agarose gel and stained with SYBR green. **(G)** Western blot showing expression of GFP-RPA32(wt), GFP-RPA32(8D) or GFP-RPA32(8A) for *Asi*SI resection assays. **(H)** Western blot showing expression of RPA32(wt)-myc, RPA32(8D)-myc or RPA32(8A)-myc for DR-HR assays. α-tubulin is a loading control. **(I)** Quantification of HR of U2OS cells transfected with I-SceI, no plasmid, or I-SceI + siRPA2. Error bars: SEM from four biological replicates. ns, $p>0.05$; * , $p<0.05$; **, $p<0.01$; ***, $p<0.001$; ****, $p<0.0001$.

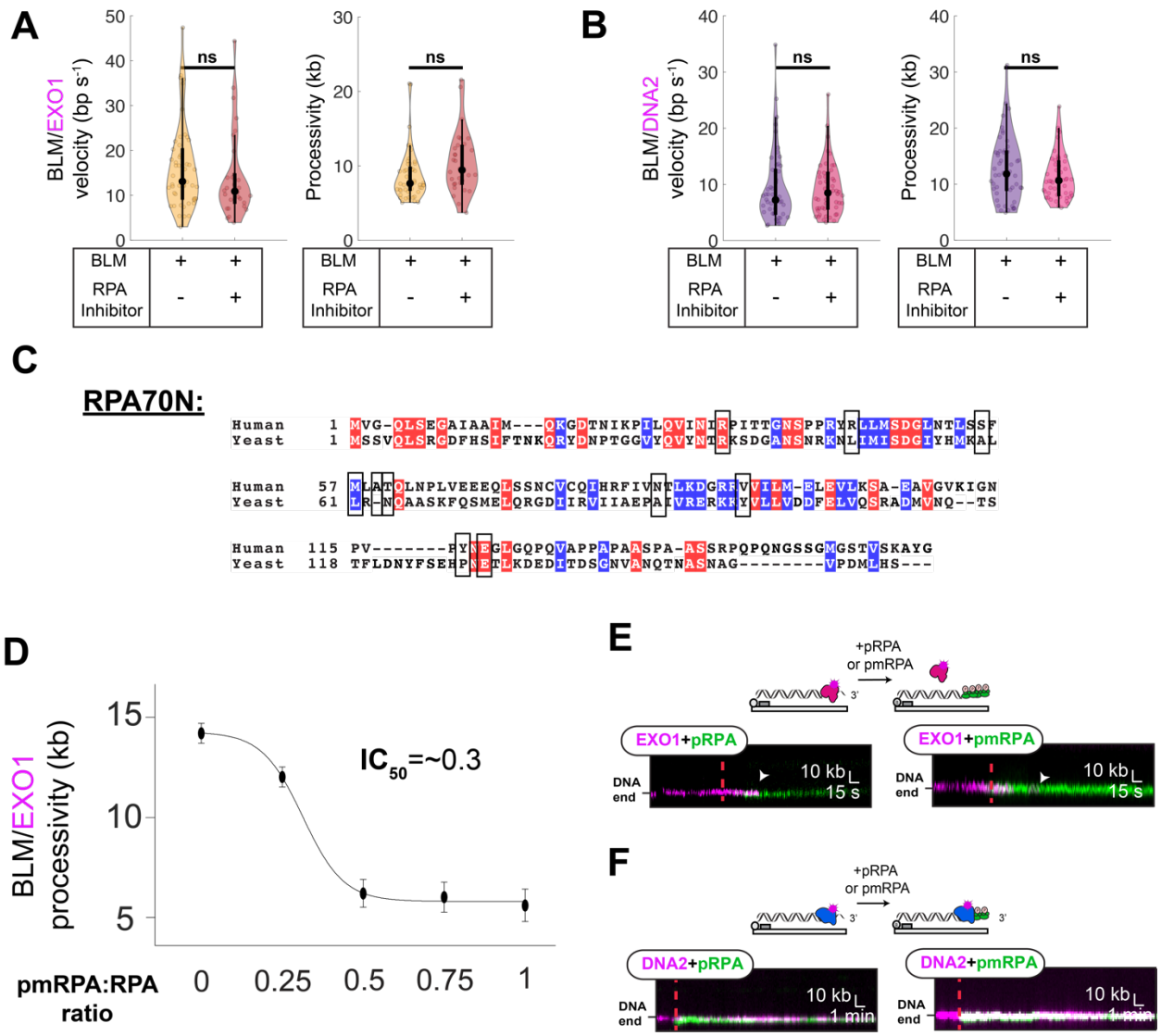

Figure S3. Characterization of RPA70N interaction with resectosomes, Related to Figure 2.

(A-B) Velocity and processivity distributions of **(A)** BLM/EXO1 (n=50 without RPA70N inhibitor; n=30 with RPA70N inhibitor) and **(B)** BLM/DNA2 (n=50 without RPA70N inhibitor; n=50 with RPA70N inhibitor) with and without RPA70N inhibitor 3,3',5,5'-tetraiodothyroacetic acid (Kang et al., 2018; Souza-Fagundes et al., 2012). The RPA inhibitor does not inhibit resection in absence of RPA. **(C)** Human and *S. cerevisiae* RPA70N sequence alignment generated by CLUSTALW2 (Larkin et al., 2007)**.** Red: identical amino acid residues; blue: conserved amino acid substitutions. Boxes represent residues important for BLM-RPA70N interactions (Kang et al., 2018). These residues are divergent between the yeast and human RPA70 proteins. **(D)** The mean

BLM/EXO1 processivity at increasing ratios of pmRPA to RPA. The data are fit to a dose-response curve indicating that ~30% pmRPA is sufficient to stall resection. Error bars: SEM**. (E)** Representative kymographs showing EXO1 is rapidly stripped from DNA in the presence of pRPA or pmRPA, as we had observed for wt RPA (Myler et al., 2016). White arrows indicate EXO1 dissociation. **(F)** Representative kymographs showing DNA2 remains on DNA but does not move within our resolution in the presence of pRPA or pmRPA.

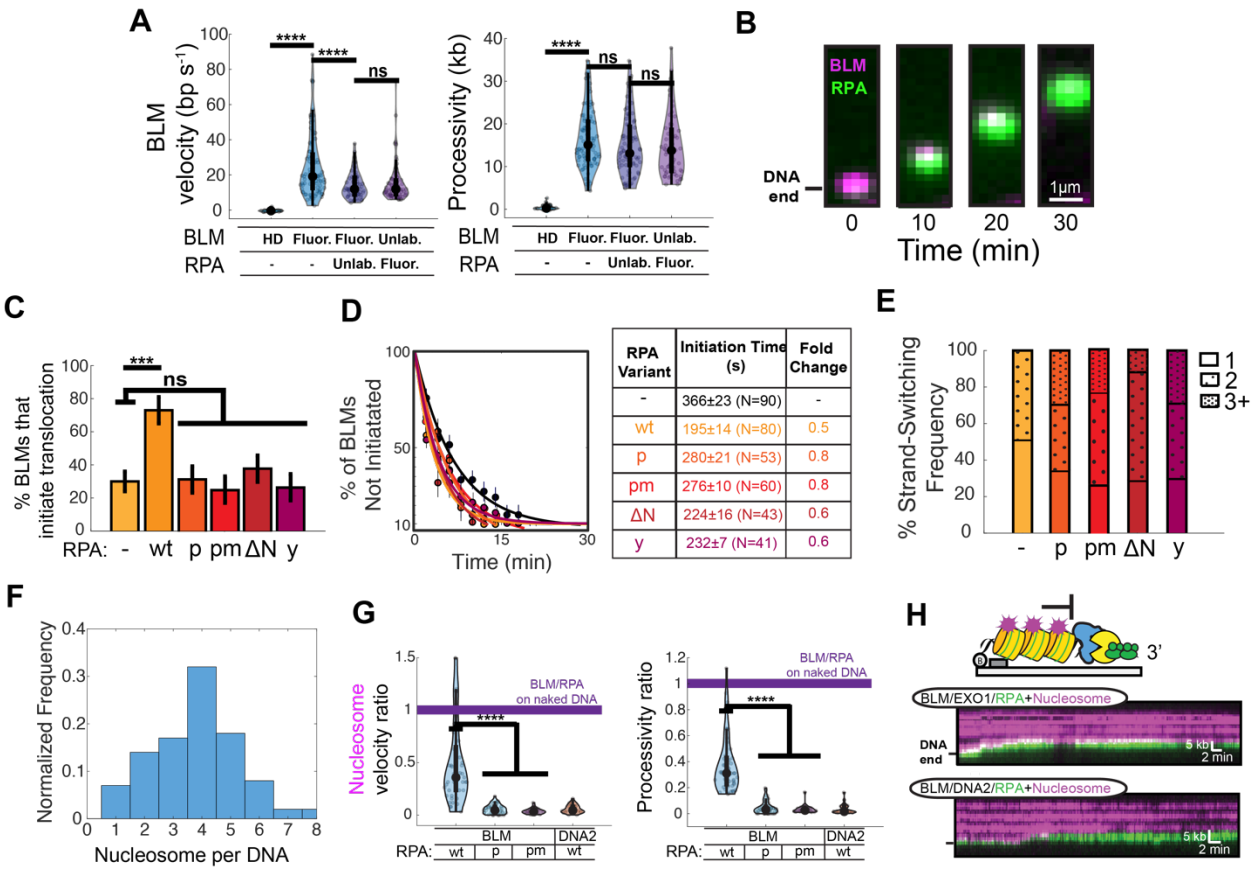

Figure S4. Characterization of RPA regulation of BLM helicase and resection on nucleosome-coated DNA, Related to Figures 3 and 4.

(A) Fluorescent BLM and unlabeled BLM have statistically indistinguishable velocities and processivities. Unlabeled BLM helicase activity was monitored via the movement of an RPA-GFP punctum. (ns, $p>0.05$; ****, $p<0.0001$). **(B)** RPA-GFP intensity increased with BLM helicase activity due to accumulation of ssDNA during BLM translocation. **(C)** RPA stimulates BLM helicase initiation. This requires BLM-RPA70N interactions. RPA variants: wt RPA (wt), pRPA (p), pmRPA (pm), RPAΔN (ΔN), and yRPA (y). Error bars: S.D. as determined by bootstrap analysis. **(D)** BLM helicase initiation analysis with RPA variants. Error bars: S.D. as determined by bootstrap analysis. **(E)** pRPA increases the strand-switching frequency of BLM helicase. **(F)** Quantification of number of nucleosomes per DNA (n=100 DNA molecules analyzed). **(G)** Relative velocity and processivity of fluorescently-labeled nucleosomes encountered by BLM/RPA (n=46), BLM/pRPA (n=48), or BLM/pmRPA (n=30). DNA2 cannot encounter nucleosomes because it is stationary on 3'-ssDNA overhangs in the absence of BLM (n=40; see

Fig. S1F). The velocity and processivity for DNA2/RPA on naked DNA are therefore compared to BLM/DNA2/RPA on naked DNA showing the requirement of BLM for DNA2-mediated resection. **(H)** Representative kymographs showing BLM/EXO1 (top) and BLM/DNA2 (bottom) in the presence of RPA (green) are able to push single nucleosomes (magenta) but stall at higher-density nucleosomal substrates.

Table S1. Oligonucleotides used in this study, Related to STAR Methods.

Name	Sequence
IF007	[p]AGG TCG CCG CCC[Bio]
LM003	[p]GGG CGG CGA CCT TTTTTTTTTTTTTTTTTTTTTTTTTTTTTTTTTTTTTTTTTTTTTTTT TTTTTTTTTTTTTTTTTTTTTTTTTTTT
siRPA2 (3'-UTR)	Sense: 5' A.A.C.C.U.A.G.U.U.U.C.A.C.A.A.U.C.U.G.U.U 3' Antisense: 5' C.A.G.A.U.U.G.U.G.A.A.A.C.U.A.G.G.U.U.U.U 3'
MS002	CATCGGACCGAGATC
MS003	GACTACAAGGATGACGACGACAAGGGCGCCATGGGATCCGCT
MS004	GTCCCGGACTATGCAGGATCCTATCCATATGACGTTCCAGATTACGGCG CCATGGGATCC
MS005	CGGGACGTCATAGGGATAGCCAGCGTAATCTGGAACATCGTATGGGTAC ATCGGACCGAG
MS006	GCGGCTACGACCAGGACCCGGGGGGCTTTGGAGACCCCGCACCTGACC AAGCCGAAAAG
MS007	CGGCTCCCCCGTAGTCGTCGTCGCCATAGTCTTCGAATCCACTGTTCCAC
MS008	CGGCTCCCCCGTAGGCGGCGGCGCCATAGGCTTCGAATCCACTGTTCCAC
MS009	GCGGCTACGCCCAGGCCCCGGGGGGCTTTGGAGCCCCCGCACCTGCCCA AGCCGAAAAG